Shadows and strong gravitational lensing

Pedro Cunha

Physics Department of the University of Aveiro and CIDMA
IST - University of Lisbon, Portugal

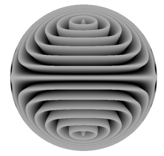

arXiv:**1808.06692**: + Herdeiro, Radu

GRG **50** no.4, 42: + Herdeiro**,** PRL **119** no.25, 251102: + Berti, Herdeiro

PRD **97** no.8, 084020: + Herdeiro, Rodriguez**,** PRD **98** 044053: + Herdeiro, Rodriguez

Can we always see the shape of a star?

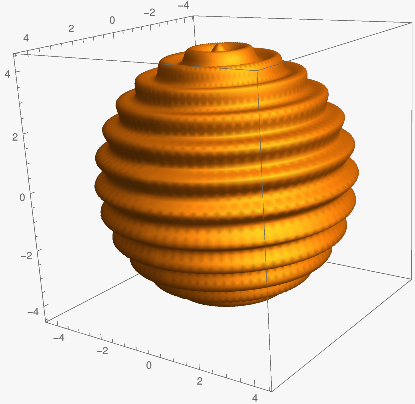

- Consider a star with a bumpy surface, and radius $R \in [R_1, R_2]$.
- The Schwarzschild solution describes the exterior of the star.
- Do we always see the same outline of the star?

Image bumpy star ($3M < R$)

If $3M < R$:

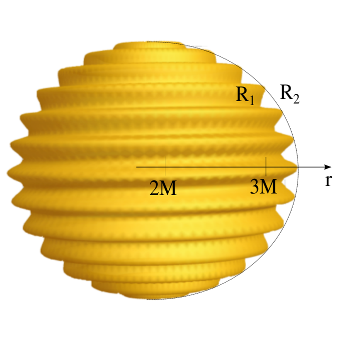

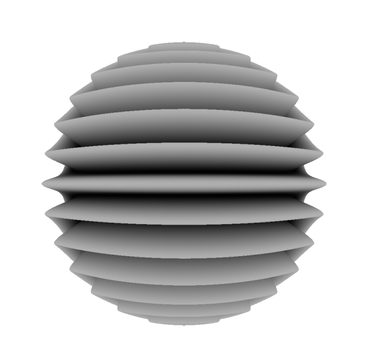

Image of the star

- The star's image is what one might expect.
- The star edge displays the bumpy surface of the star.

Image bumpy star ($3M < R$)

If $3M < R$:

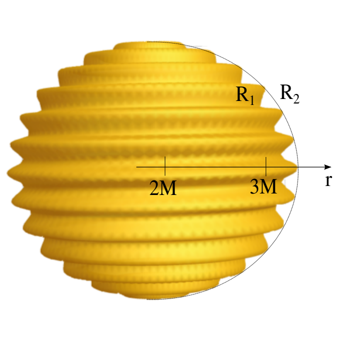

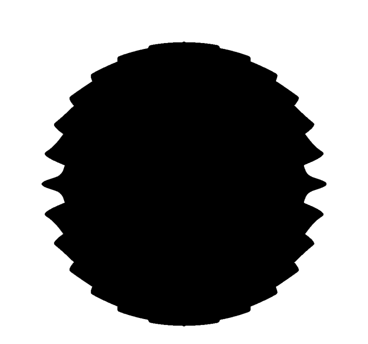

Image of the star (no emission)

- Black star $\rightarrow$ radiation absorbent and no emission.
- If the star is black, only the outline contains surface information.

Image bumpy star ($R < 3M$)

If $R < 3M$:

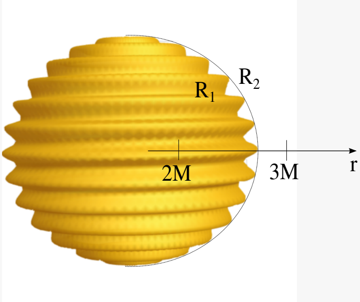

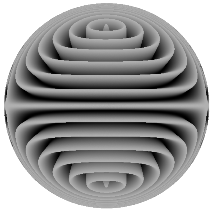

Image of the star

- The star's edge becomes circular (no display of the bumpy surface).
- The edge is actually an image of the photon sphere ($r = 3M$).

Image bumpy star ($R < 3M$)

If $R < 3M$:

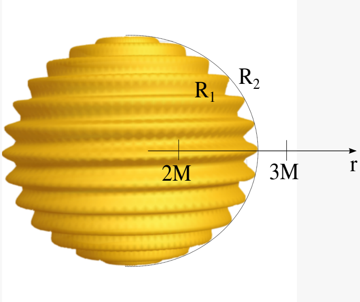

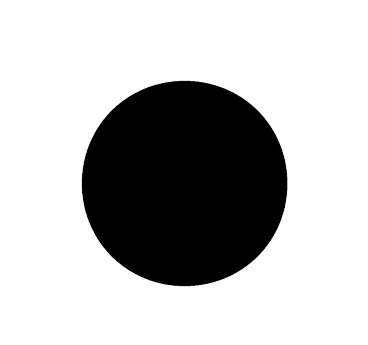

Image of the star (no emission)

- A black star image reveals no surface information.
- This image coincides with the *shadow* of a BH.

Backwards ray-tracing

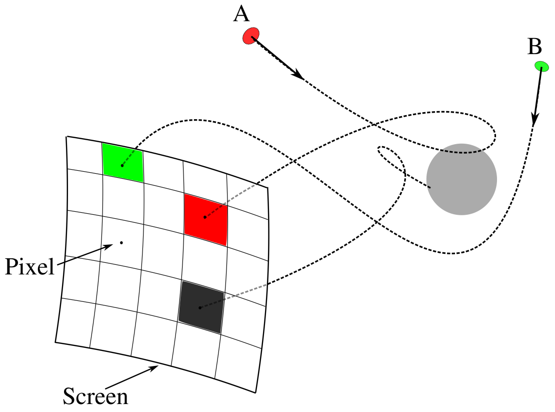

- Image defined as a grid of pixels in the observer's screen.
- Each pixel defines an initial condition for a light ray.
- *Shadow* $\rightarrow$ set of pixels with rays infalling into a BH.

Shadows of BHs

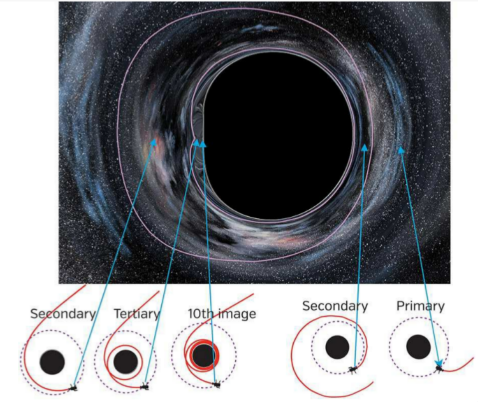

Adapted K.Thorne.

- The edge of the shadow corresponds to a scattering singularity.
- Photons encircle the black hole an increasing number of times.
- The shadow edge is determined by a special class of orbits.

Light rings

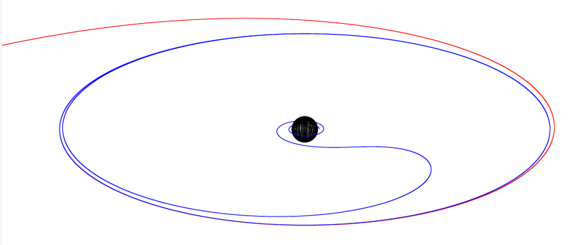

- *Light ring* (LR) $\iff$ circular photon orbit.
- Tangent vector field is a linear combination of (only) $\partial_t, \partial_\varphi$.
- Killing vectors $\partial_t, \partial_\varphi$ connected to stationarity and axial-symmetry.
- Kerr has *two* unstable LRs with opposite rotation.

Spherical photon orbits (Kerr)

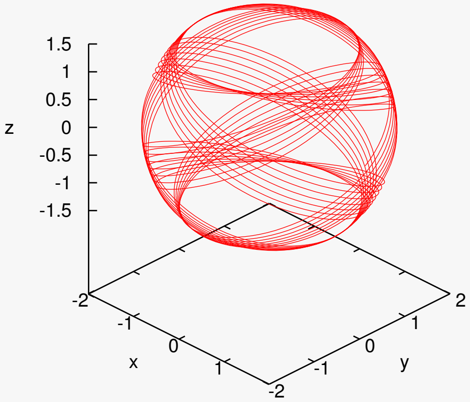

- Kerr → Light rings generalize outside the equatorial plane.
- In Boyer-Lindquist coordinates → orbits with constant r.

Geodesic motion

- The Hamiltonian $\mathcal{H}$ of geodesic motion does not depend on t, φ:

$$\frac{\partial \mathcal{H}}{\partial x^\mu} = -\dot{p}_\mu \quad \Longrightarrow \text{ constant} \quad p_t,\, p_\varphi$$

- Constants of photon motion:

$$E = -p_t \qquad \rightarrow \text{energy at infinity}$$
$$L = p_\varphi \qquad \rightarrow \text{angular momentum}$$

- Motion depends on the impact parameter $\eta = L/E$.

Spherical photon orbits (Kerr)

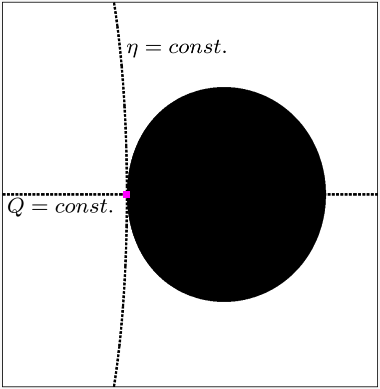

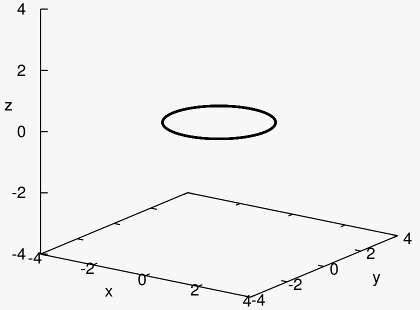

- Besides η there is another constant of motion (Carter's Q).
- Each spherical orbit is uniquely identified by $\{\eta, Q\}$.
- Spherical orbits determine the Kerr shadow edge.

Spherical photon orbits (Kerr)

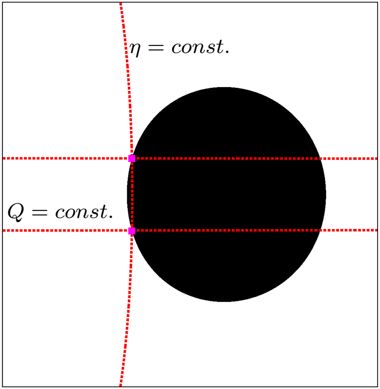

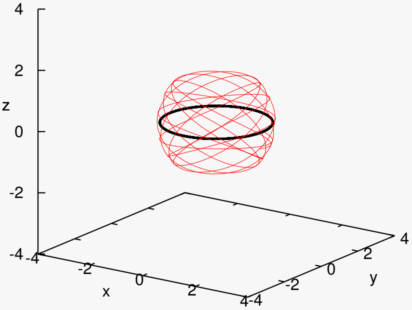

- Besides η there is another constant of motion (Carter's Q).
- Each spherical orbit is uniquely identified by $\{\eta, Q\}$.
- Spherical orbits determine the Kerr shadow edge.

Spherical photon orbits (Kerr)

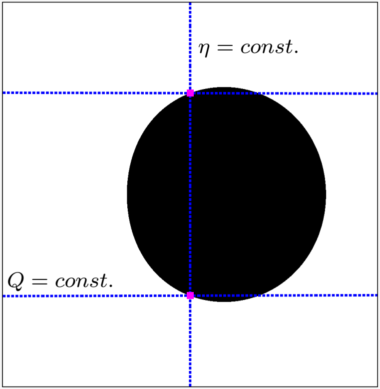

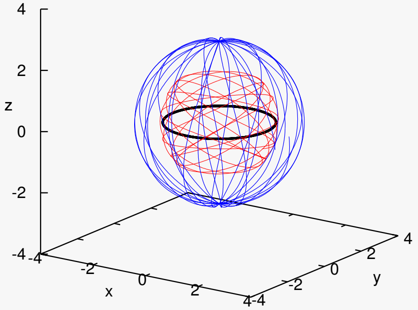

- Besides η there is another constant of motion (Carter's Q).
- Each spherical orbit is uniquely identified by $\{\eta, Q\}$.
- Spherical orbits determine the Kerr shadow edge.

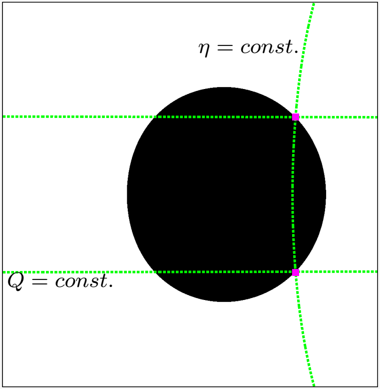

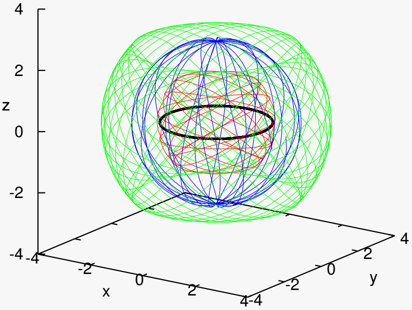

- Besides η there is another constant of motion (Carter's Q).
- Each spherical orbit is uniquely identified by $\{\eta, Q\}$.
- Spherical orbits determine the Kerr shadow edge.

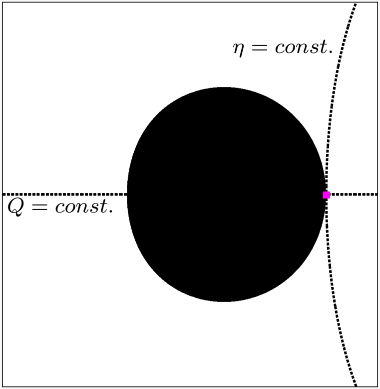

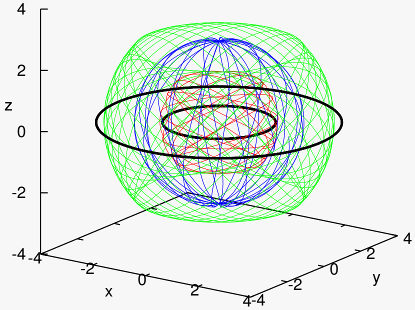

- Besides η there is another constant of motion (Carter's Q).
- Each spherical orbit is uniquely identified by $\{\eta, Q\}$.
- Spherical orbits determine the Kerr shadow edge.

Analytic Kerr shadow

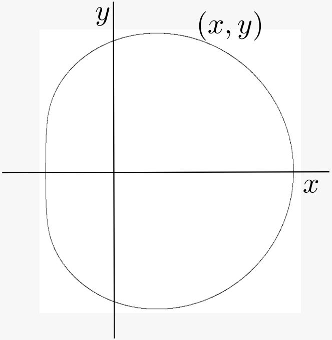

- The Kerr shadow edge $\{x(r)\,,\,y(r)\}$ is known analytically.
- The parameter r is the spherical photon orbit radius.
- Is it possible to represent $y(x)$ directly?

Analytic Kerr shadow

- Consider an observer with $r_{obs} \gg 1$.
- The Kerr spin is a. For simplicity, if $\theta_{obs} = \pi/2$:

$$y = \pm\sqrt{\frac{r^2(3r^2 + a^2 - x^2)}{r^2 - a^2}}$$

- The parameter r satisfies the cubic equation:

$$r^3 - 3r^2 + a(a - x)r + a(a + x) = 0$$

Analytic Kerr shadow

- The solution has three branches (in M units):

$$\mathcal{A} \equiv 1 - \frac{a}{3}(a - x), \qquad \mathcal{B} \equiv \frac{(1 - a^2)}{|\mathcal{A}|^{3/2}}.$$

If $\mathcal{A} > 0, \quad \mathcal{B} \leqslant 1$:

$$\boxed{r = 1 + 2\sqrt{\mathcal{A}} \cos\left(\frac{1}{3} \arccos \mathcal{B}\right)}$$

If $\mathcal{A} \geqslant 0, \quad \mathcal{B} > 1$:

$$\boxed{r = 1 + 2\sqrt{\mathcal{A}} \cosh\left(\frac{1}{3} \log\left[\sqrt{\mathcal{B}^2 - 1} + \mathcal{B}\right]\right)}$$

If $\mathcal{A} < 0$:

$$\boxed{r = 1 - 2\sqrt{|\mathcal{A}|} \sinh\left(\frac{1}{3} \log\left[\sqrt{1 + \mathcal{B}^2} - \mathcal{B}\right]\right)}$$

Analytic Kerr shadow

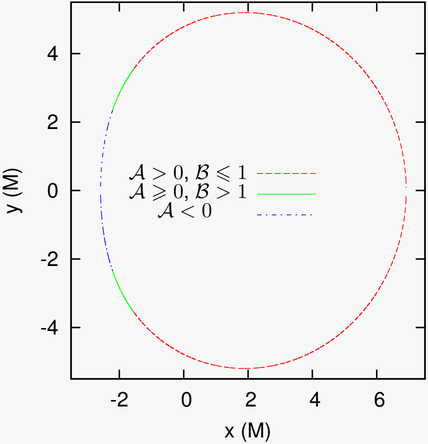

- Kerr shadow edge function $y(x)$ for $a = 0.95$.
- All three branches are necessary to cover the entire edge.
- The observer is at infinity and in the equatorial plane.

Extreme Kerr shadow ($a = 1$)

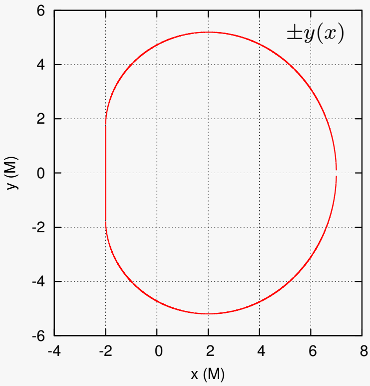

$(a = 1)$

- Extremal limit $\rightarrow$ shadow expression simplifies considerably:

$$\boxed{y(x) = \sqrt{11 + 2x - x^2 + 8\sqrt{2 + x}}}, \qquad -2 < x \leqslant 7$$

Event Horizon Telescope

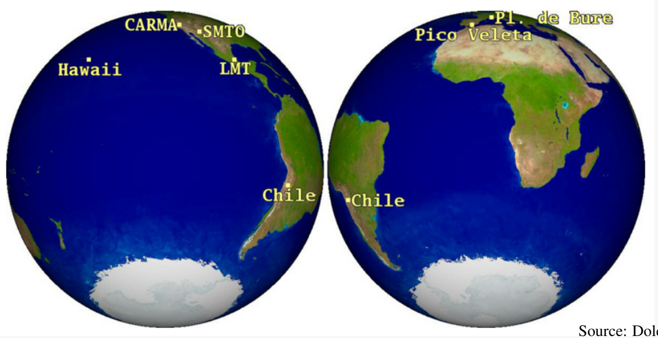

Source: Doleman et al.

- The shadow of a BH is a direct observable.
- The EHT collaboration aims to capture the first BH shadow.
- Network of VLBI stations $\rightarrow$ creates a virtual Earth-sized telescope.

Kerr's Spherical Photon orbits revisited

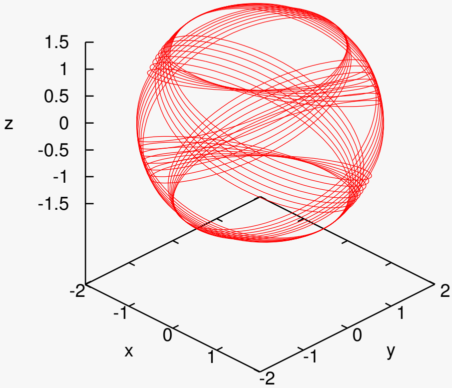

- The geodesic motion is completely integrable in Kerr.
- There are special orbits with constant $r \rightarrow$ Spherical Photon Orbits.
- This is not a invariant statement that can be used generically.

Fundamental photon orbits (FPOs)

A null geodesic curve $s(\lambda) : \mathbb{R} \to \mathcal{M}$ is a *fundamental orbit* if:

$\rightarrow$ it is restricted to a spatial region;
$\rightarrow$ there is a value $T > 0$ for which $s(\lambda) = s(\lambda + T), \qquad \forall \, \lambda \in \mathbb{R}$

up to isometries.

- These orbits are not required to be periodic on the manifold $\mathcal{M}$.
- They are periodic on $\{r, \theta\}$ (not connected to Killing vectors).
- These orbits can exist even if the geodesics are *not* fully integrable.

Example: BHs with Proca hair

Stable

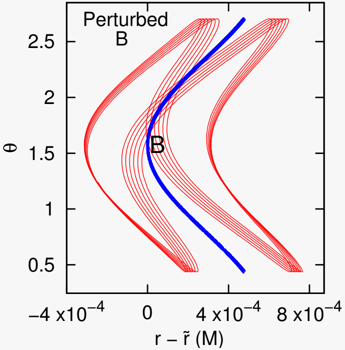

Unstable

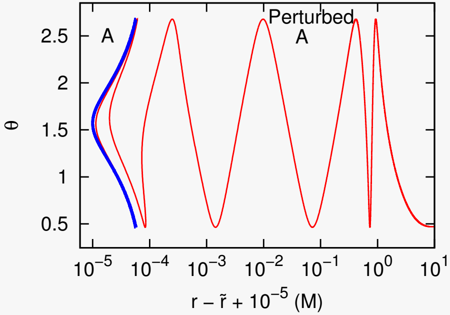

- Example of FPOs (in blue) and their perturbations (red).
- Each orbit can be labeled by the value of r on the equatorial plane.
- Their stability can analysed by taking $\theta = \pi/2$ as a *Poincaré section*.

Example: Shadow cusp in BHs with Proca hair

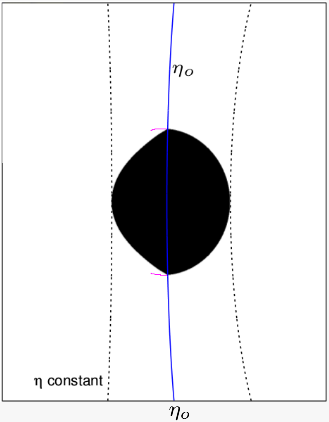

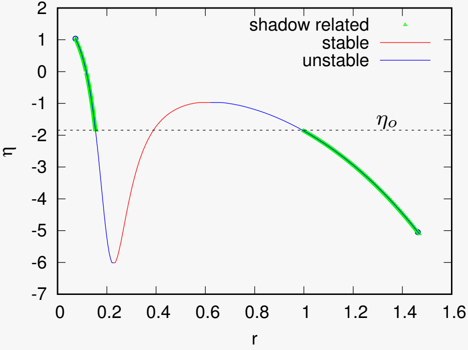

- Plot displays a continuous family of fundamental orbits (FPOs).
- *Cusp* on shadow edge $\rightarrow$ transition between unstable orbits.
- This a non Kerr-like feature $\rightarrow$ consequence different FPO structure.

Example: Einstein-dilaton-Gauss-Bonnet (EdGB)

Einstein-dilaton-Gauss-Bonnet model

$$S = \frac{1}{16\pi}\int d^4x\sqrt{-g}\left[R - \frac{1}{2}(\partial_\mu\phi)^2 + \alpha e^{-\gamma\phi}R^2_{\mathrm{GB}}\right].$$

The Gauss-Bonnet term (2^{nd} Euler density) is:

$$R^2_{GB} = R_{\mu\nu\rho\sigma}R^{\mu\nu\rho\sigma} - 4R_{\mu\nu}R^{\mu\nu} + R^2$$

- R_{GB} gives a dynamic contribution when coupled to scalar field ϕ.
- BH solutions can have *exotic effective matter* close to the horizon.

Cunha+ PLB 768 373-379

Example: Einstein-dilaton-Gauss-Bonnet (EdGB)

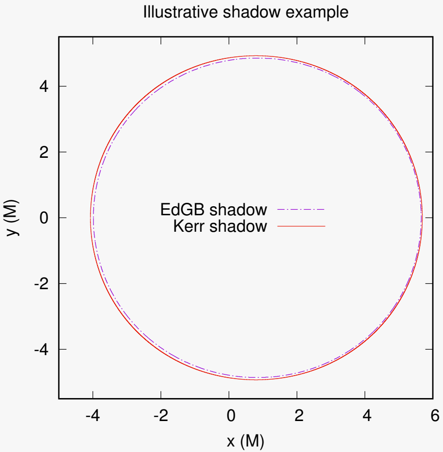

- Non-trivial horizon physics is cloaked by the shadow!
- The structure of fundamental photon orbits (FPOs) is very Kerr-like.
- Shadow observations are unlikely to exclude EdGB models.

Example: Kerr shadow sketch

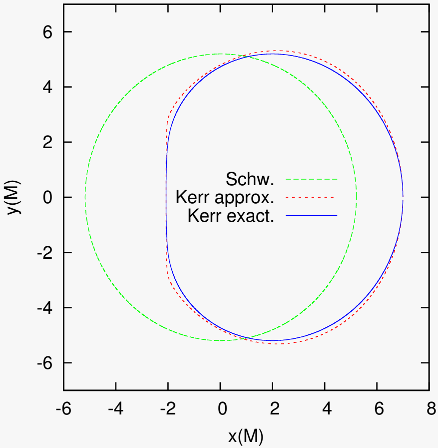

- One can develop an approximate method to obtain a shadow.
- Contribution of each FPO $\rightarrow$ similar to a Schwarzschild FPO.
- Manages to capture the main features of the Kerr shadow.

Light rings (revisited)

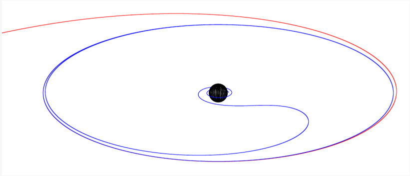

- *Light ring* (LR) $\to$ assign a topological charge.
- We can introduce 2D effective potential $U(r, \theta)$.
- Along trajectory $p_r = p_\theta = U = 0$ and $\dot{p}_\mu = 0$.
- $2\,\dot{p}_\mu = -\partial_\mu U + \mathcal{O}(p_r,\, p_\theta)$.

At a LR: $\Longrightarrow$ $\boxed{U = \nabla U = 0}$

Effective potentials

- Shortcoming of $U \rightarrow$ depending on parameters E, L.
- Can be factorized as $U = (L^2 g^{tt})(\sigma - H_+)(\sigma - H_-), \qquad \sigma \equiv E/L.$

At a LR: $\Longrightarrow$ $\boxed{\nabla H_\pm = 0}$ (critical point of $H_\pm$)

$\rightarrow$ Next: we assign a topological quantity to a LR.

Winding number

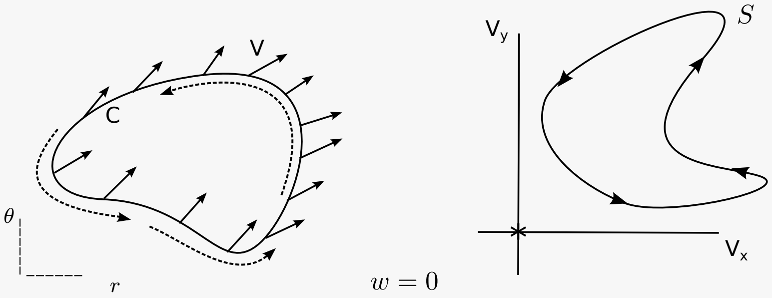

- Consider a closed 2D contour C with a 2D field $V = \nabla H_{\pm}$.
- The circulation of V around C is mapped to a curve $S(V_x, V_y)$.
- The winding number around $V = 0$ is a topological quantity w.

Winding number

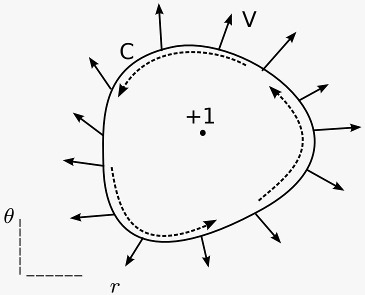

$w = +1$

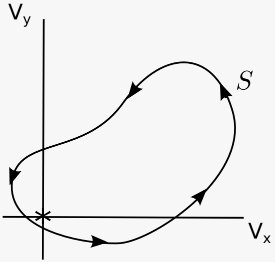

- Consider a closed 2D contour C with a 2D field $V = \nabla H_{\pm}$.
- The circulation of V around C is mapped to a curve $S(V_x, V_y)$.
- The winding number around $V = 0$ is a topological quantity w.

Winding number

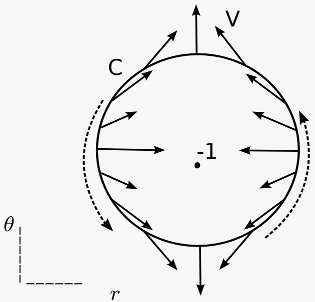

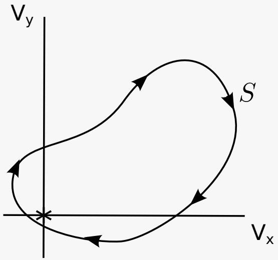

$w = -1$

- Consider a closed 2D contour C with a 2D field $V = \nabla H_{\pm}$.
- The circulation of V around C is mapped to a curve $S(V_x, V_y)$.
- The winding number around $V = 0$ is a topological quantity w.

Light Ring types

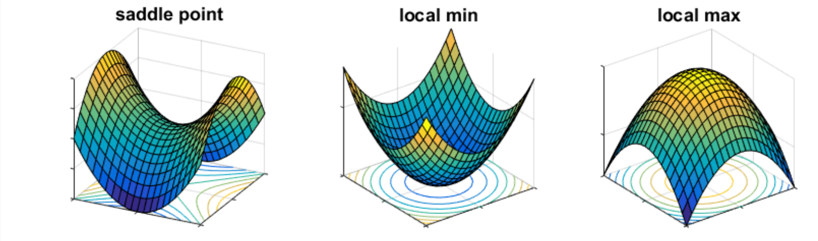

$w = -1$ $\qquad$ $w = +1$ $\qquad$ $w = +1$

Different types of LRs:

- Saddle point of U $\rightarrow$ unstable LR $(w = -1)$ $\rightarrow$ Kerr, GW ringdown.
- Local minimum of U $\rightarrow$ stable LR $(w = +1)$ $\rightarrow$ spacetime instability.
- Local maximum of U $\rightarrow$ unstable LR $(w = +1)$ $\rightarrow$ violates NEC.

Illustration Brouwer degree w

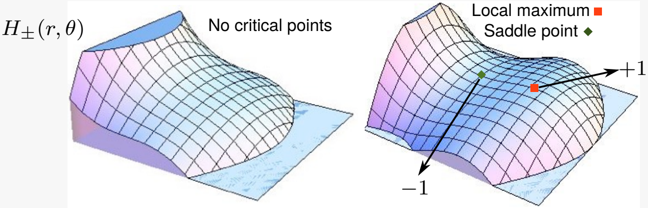

$w = 0$ $\qquad$ $w = 0$

Smooth deformation of $H_{\pm}(r,\theta)$ (fixed asymptotics):

- Total w is a constant.
- LRs are created in pairs.

Example: Proca Stars

$\simeq$ flat spacetime $\rightarrow$

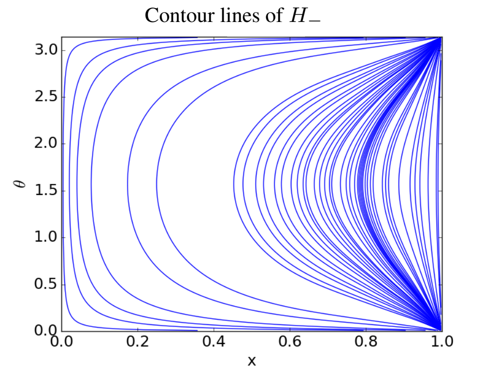

$x \equiv r/(1+r)$

- Continuous families of spacetimes: Proca and Boson Stars.
- Sequence of solutions $\rightarrow$ deformation of $H_\pm$.
- Flat spacetime $\neq$ flat $H_\pm$

Example: Proca Stars

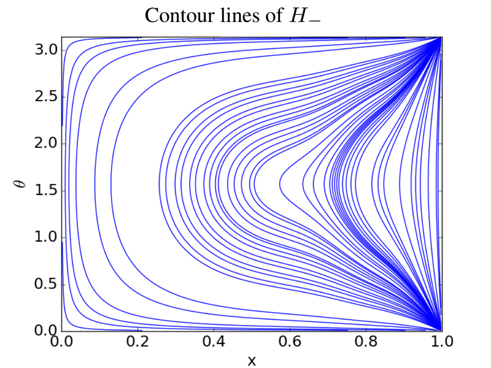

$x \equiv r/(1+r)$

- Continuous families of spacetimes: Proca and Boson Stars.
- Sequence of solutions $\rightarrow$ deformation of $H_{\pm}$.
- Flat spacetime $\neq$ flat $H_{\pm}$

Example: Proca Stars

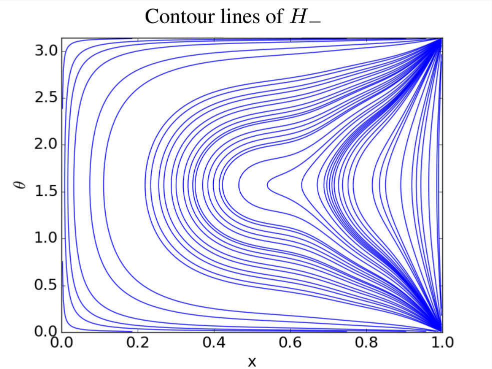

$x \equiv r/(1+r)$

- Continuous families of spacetimes: Proca and Boson Stars.
- Sequence of solutions $\rightarrow$ deformation of $H_\pm$.
- Flat spacetime $\neq$ flat $H_\pm$

Example: Proca Stars

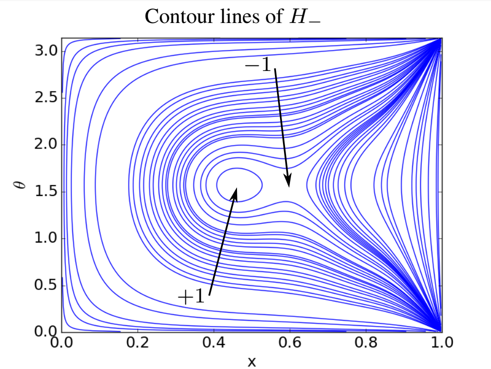

$x \equiv r/(1+r)$

- Continuous families of spacetimes: Proca and Boson Stars.
- Sequence of solutions $\rightarrow$ deformation of $H_{\pm}$.
- Flat spacetime $\neq$ flat $H_{\pm}$

Example: Proca Stars

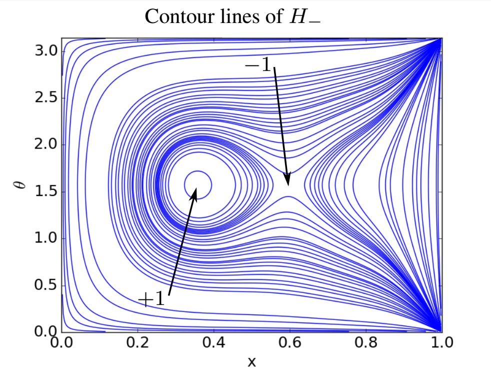

$x \equiv r/(1+r)$

- Continuous families of spacetimes: Proca and Boson Stars.
- Sequence of solutions $\rightarrow$ deformation of $H_\pm$.
- Flat spacetime $\neq$ flat $H_\pm$

Example: Majumdar-Papapetrou binary (MP)

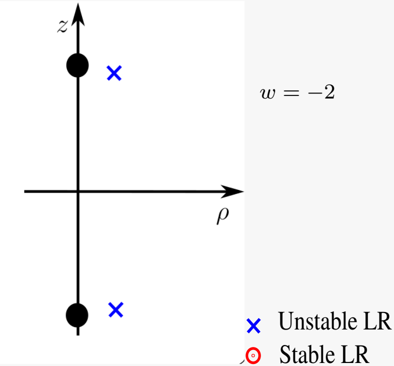

- The MP binary describes two maximally charged BHs in equilibrium.
- In the large separation limit $\rightarrow$ each BH has an unstable LR.

Example: Majumdar-Papapetrou binary (MP)

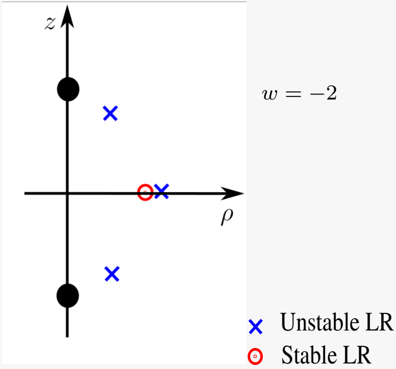

- The MP binary describes two maximally charged BHs in equilibrium.
- By reducing the separation between the BHs $\rightarrow$ a stable LR forms.

Example: Majumdar-Papapetrou binary (MP)

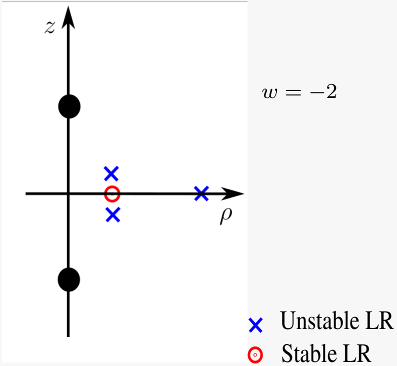

- The MP binary describes two maximally charged BHs in equilibrium.
- By reducing the separation between the BHs $\rightarrow$ a stable LR forms.

Example: Majumdar-Papapetrou binary (MP)

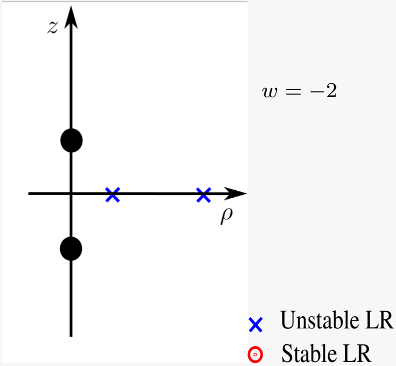

- The MP binary describes two maximally charged BHs in equilibrium.
- Two unstable LRs created with different stability orientations.

Shadow BH binary

Bohn+ CQG 065002

- The shadow of a dynamical BH binary is computationally expensive.
- Is it possible to obtain a binary shadow proxy from a static solution?

Double Schwarzschild solution

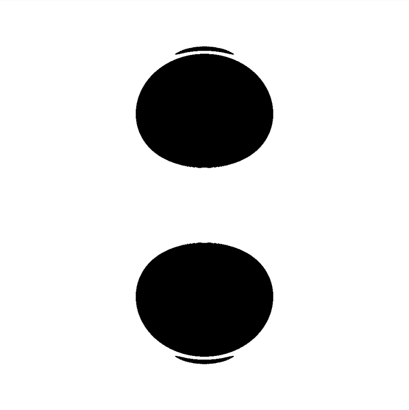

- One can start from the (static) 2-Schwarzschild vacuum solution.
- Describes two equal BHs hold in equilibrium by a conical singularity.
- Both BHs are uncharged, and the solution is axially symmetric.

Double Schwarzschild solution

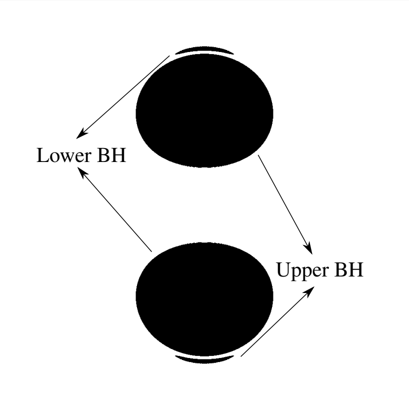

- The shadow is disconnected: there are multiple components.
- Despite the conical singularity, the shadows are smooth.
- Could we mimic the rotation of a binary?

Quasi-static binary

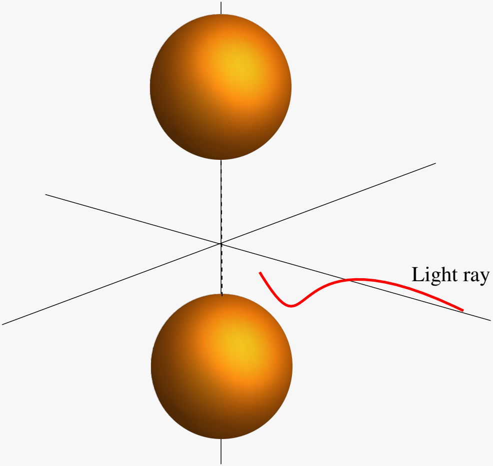

- Assume that BHs move much slower than light rays.
- We can then implement a quasi-static approximation.

Quasi-static binary

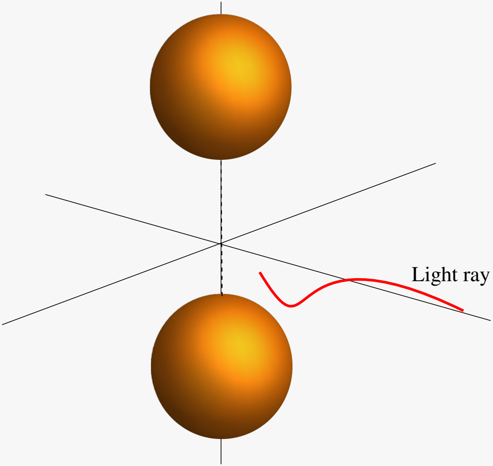

- At first order $\rightarrow$ light rays follow geodesics in the static background.
- By making periodic rotations we can account for the BHs' motion.

Quasi-static binary

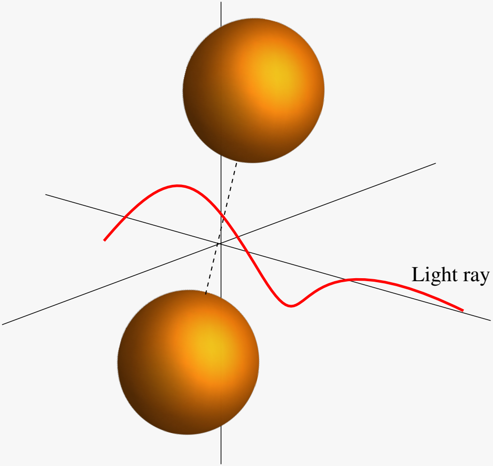

- At first order $\rightarrow$ light rays follow geodesics in the static background.
- By making periodic rotations we can account for the BHs' motion.

Quasi-static binary

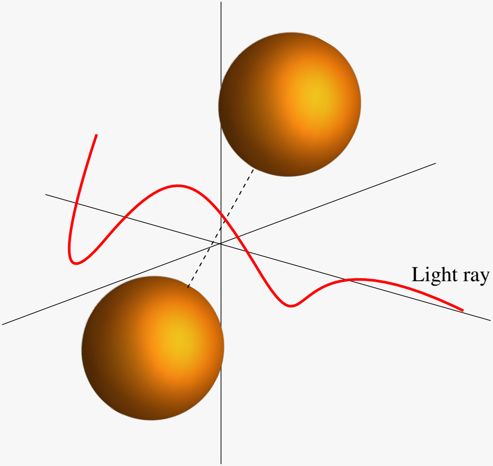

- At first order $\rightarrow$ light rays follow geodesics in the static background.
- By making periodic rotations we can account for the BHs' motion.

Shadows Quasi-static binary

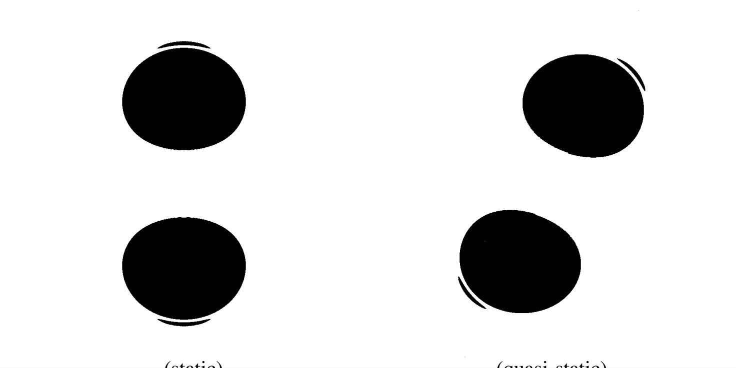

(static) (quasi-static)

- Using this naive rotation, the shadows are modified.
- The secondary shadows are displaced with respect to the primary ones.

Fully numerical *vs.* Quasi-static

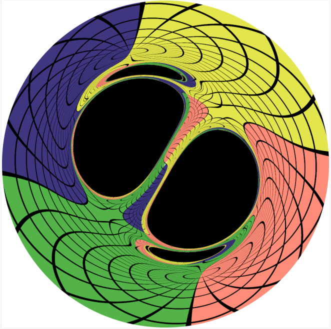

(fully numerical)
Bohn+ CQG 065002

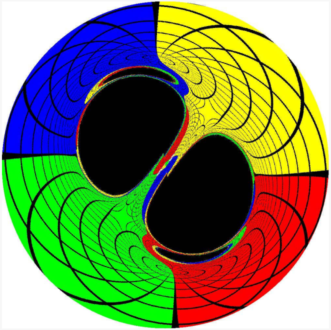

(quasi-static)
Cunha+ PRD 98 044053

- One can compare the approximation with the fully numerical result.
- Despite some differences, the resemblance is uncanny.

Recent results: shadows of the Rasheed solution

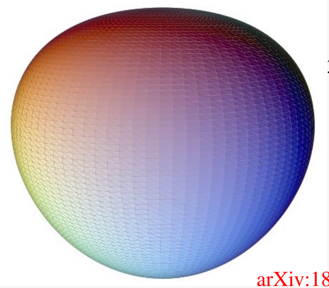

3D horizon embedding

arXiv:1808.06692

- This solution is stationary, axially-symmetric and asymptotically flat.
- Kaluza-Klein rotating dyonic BHs $\rightarrow$ generically not $\mathbb{Z}_2$ symmetric.
- The horizon can be North-South asymmetric.

Recent results: shadows of the Rasheed solution

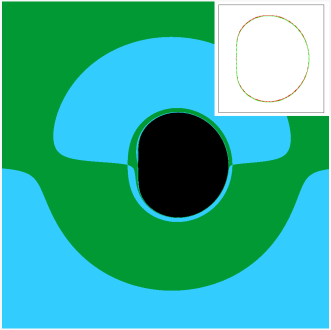

Observer at $\theta = \pi/2$.

- The lensing is not $\mathbb{Z}_2$ symmetric (no color permutation invariance).
- However, the shadow is always $\mathbb{Z}_2$ symmetric!
- The FPO structure is still much Kerr-like.

arXiv:1808.06692

Recent results: BH rocket

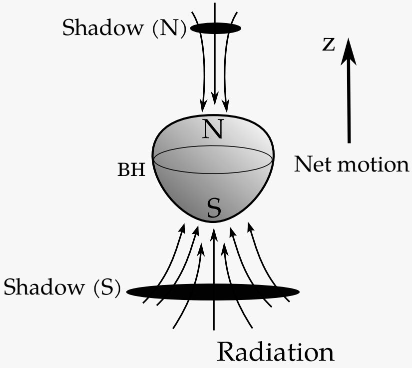

- The shadow size is not the same as seen from the North (South) pole.
- Infalling radiation can lead to asymmetric momentum absorption.
- This would lead to a spontaneous thrust: a *BH rocket* effect!

arXiv:1808.06692

Conclusions

- The FPOs determine the shadow edge of BHs.
- These orbits can exist even if the geodesic motion is not separable.
- Very different phenomenology $\rightarrow$ very different FPO structure.

Acknowledgements

- Work is supported by the FCT IDPASC Portugal Ph.D. Grant No. PD/BD/114071/2015 and partially supported by the H2020-MSCA-RISE2015 Grant No. StronGrHEP-690904, the H2020-MSCA-RISE-2017 Grant No. FunFiCO-777740 and by the CIDMA project UID/MAT/04106/2013.